International Journal of Heat and Technology
Vol. 36, No. 1, March, 2018, pp. 353-358
Journal homepage: http://iieta.org/Journals/IJHT

Heat transfer of the TiO_2/water nanofluid in an annulus of the finite rotating cylinders

M. R. A. Rahman[1*], M. R. Saad[1], A. C. Idris[1], H. M. Faizal[2]

[1] Department of Mechanical Engineering, Faculty of Engineering, Universiti Pertahanan Nasional Malaysia, Kem Sg. Besi, 57000 Kuala Lumpur, Malaysia
[2] Automotive Development Centre, Faculty of Mechanical Engineering, Universiti Teknologi Malaysia, 81310, Johor, Malaysia

Corresponding Author Email: rosdzimin@gmail.com

https://doi.org/10.18280/ijht.360147

Received: 21 June 2017
Accepted: 12 March 2018

Keywords:
nanofluid, finite rotating annulus, co-rotating, counter rotating

ABSTRACT

Study on the heat transfer of TiO_2/water nanofluid flows inside annulus of the finite rotating cylinders was done numerically. Inner shaft and outer tube were rotated in co-rotating and counter-rotating direction. The k-epsilon turbulent model and the Mixture-multiphase model were used to treats the turbulence flow and the multiphase flows of the TiO_2/water nanofluid, respectively. Results of the current work are in agreement with published work. Results showed that increased in Reynolds number the Nusselt number increases. The distribution of the Nusselt number at the specific location along the heated inner shaft for co-rotating and counter-rotating cases shows a different distribution profile. The counter-rotating case was found to be more efficient in enhancing the heat transfer rate in comparison to the co-rotating case. This observation is suggested because of the boundary layers disturbances that originate from the additional vortices produced by the competing rotational speed between inner shaft and outer tube.

1. INTRODUCTION

Flow in an annulus of two concentric rotating cylinders is known as the Taylor-Couette-Poiseuille flow. This type of flow is important for the study of rotating shaft involving heat transfer. Heat transfer in rotating shaft is a crucial issue since the lubrication oil needs a certain working temperature to make it work at optimum level. Thus, by understanding the heat transfer behaviour in an annulus, it will help to lubricate rotating shaft efficiently. An experimental work to elucidate the heat transfer behaviour of an annulus is difficult due to a narrow gap of the annulus. Hence, a numerical simulation turns out to be a powerful tool to elucidate the heat transfer behaviour of flow in an annulus.

Water and air were used as a working fluid in previous heat transfer studies of an annulus and found that the Reynolds number [1] and the flow structure [2] are significantly influencing the heat transfer characteristics. Water and air exhibit low thermal properties, whereby for a good heat transfer process, the working fluids must possess high thermal conductivity values. The thermal conductivity of the fluid can be enhanced using nanoparticles [3]. A significant heat transfer enhancement was observed when particles at nanometres size were added into conventional fluids (water, ethylene glycol and oil), which were eventually called nanofluids [3]. Many studies on nanofluids were done to investigate the effect of particle sizes, types, volume percentages, weight percentages, type of based fluid and its application in heat exchanger [4-10]. A study using Al_2O_3-water nanofluid shows that heat transfer increased by 25.5% when 2.5 vol % of Al_2O_3 nanoparticles was added into the pure water [7].

Study on the heat transfer characteristics using nanofluid as a working fluid inside an enclosure of the infinite rotating cylinder found that the heat transfer enhancement and flow circulation were strongly depend upon the rotation speed of an ordinary shaft size placed at the center of an enclosure and also the nanoparticle concentration [11]. Moreover, increase in an average Nusselt number as increases in the cylinder size of the mixed convection case for various Richardson number was observed [12]. Furthermore, the nanoparticle volume fraction [13]-[16], cylinder rotation speed [16]-[18] and the Reynolds number [17]-[19] were found significantly influenced the heat transfer rate of rotating cylinder. In spite of the enhancement in the heat transfer rate, increases in the thickness of thermal boundary layer was also observed as the effect of the increment in the nanoparticle volume/weight fraction for infinite single rotating tube [19]-[21]. The Nusselt number is decrease as increases in drag due to the rotation of the tube [22].

Previously, studies on the heat transfer of rotating cylinders using nanofluid was focused on forced, natural and mixed convection of the infinite cylinder length. In the authors' knowledge, no study on heat transfer has been conducted in an annulus of finite length with independently rotating cylinders using nanofluid as a working fluid. Therefore, the objective of this study is to investigate numerically the heat transfer characteristiss of TiO_2/water nanofluid inside an annulus of finite length independently rotating cylinders.

2. NUMERICAL WORKS

Figures 1 and 2 show the geometry of the cylinders with a L/D_H = 60. A uniform velocity is assigned at the inlet and is used to calculate the Reynolds number. A fully developed flow is assumed at the outlet with all derivatives are zero.

Walls of the inner shaft and outer tube are rotating with non-slip condition and the inner shaft is heated with a constant heat flux. This simulation is conducted in a turbulent region and the gravity was neglected.

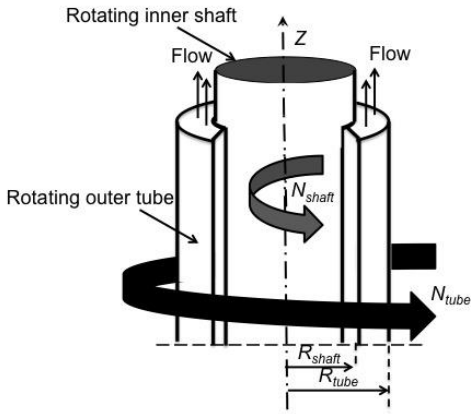

Figure 1. Geometry of the study

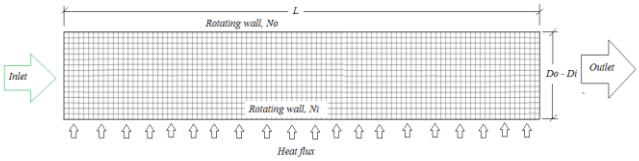

Figure 2. Numerical domain with respective boundary condition

The conservation equations were solved using Ansys FLUENT 15.0. Uniform size grid of 1×10^{-5} m $\times$ 1×10^{-5}m was used. The mixture multiphase model [21]-[23] is employed to treat the nanoparticle and water. In the mixture multiphase model, the conservation equations are solved independently. The secondary phase is solved using volume fraction equation and the relative velocity of the particle to the base fluid is calculated using algebraic expression. The steady state continuity equation is given as;

$$\nabla\cdot\left(\phi_p\rho_p+\phi_f\rho_f\frac{\phi_p\rho_p\vec{v}_p+\phi_f\rho_f\vec{v}_f}{\phi_p\rho_p+\phi_f\rho_f}\right)=0 \tag{1}$$

where $\vec{v}_p$ is the particle velocity, $\vec{v}_f$ is the base fluid velocity.

The steady state momentum equation is given as;

$$\begin{aligned}\left(\phi_p\rho_p+\phi_f\rho_f\right)&\left(\frac{\phi_p\rho_p\vec{v}_p+\phi_f\rho_f\vec{v}_f}{\phi_p\rho_p+\phi_f\rho_f}\cdot\nabla\left(\frac{\phi_p\rho_p\vec{v}_p+\phi_f\rho_f\vec{v}_f}{\phi_p\rho_p+\phi_f\rho_f}\right)\right)\\&=-\nabla P\\&+\mu_f\left[\nabla\left(\frac{\phi_p\rho_p\vec{v}_p+\phi_f\rho_f\vec{v}_f}{\phi_p\rho_p+\phi_f\rho_f}\right)\right.\\&\left.+\left(\nabla\left(\frac{\phi_p\rho_p\vec{v}_p+\phi_f\rho_f\vec{v}_f}{\phi_p\rho_p+\phi_f\rho_f}\right)\right)^T\right]\\&+\nabla\cdot\left(\phi_p\rho_p\left(\vec{v}_p-\frac{\phi_p\rho_p\vec{v}_p+\phi_f\rho_f\vec{v}_f}{\phi_p\rho_p+\phi_f\rho_f}\right)\right.\\&\left.+\phi_f\rho_f\left(\vec{v}_f-\frac{\phi_p\rho_p\vec{v}_p+\phi_f\rho_f\vec{v}_f}{\phi_p\rho_p+\phi_f\rho_f}\right)\right)\end{aligned} \tag{2}$$

The steady state energy equation is given as;

$$\nabla\cdot\left(\phi_p\vec{v}_p\rho_p h_p+\phi_f\vec{v}_f\rho_f h_f\right)=\nabla\cdot\left(k_{eff}\nabla T\right) \tag{3}$$

where h_p and h_i are the enthalphy of particles and base fluid respectively. The nanofluid effective thermal conductivity is k_{eff}.

The volume fraction equation is given as;

$$\begin{aligned}\nabla\cdot\left(\phi_p\rho_p\frac{\phi_p\rho_p\vec{v}_p+\phi_f\rho_f\vec{v}_f}{\phi_p\rho_p+\phi_f\rho_f}\right)&\\=-\nabla\cdot\left(\phi_p\rho_p\left(\vec{v}_p-\frac{\phi_p\rho_p\vec{v}_p+\phi_f\rho_f\vec{v}_f}{\phi_p\rho_p+\phi_f\rho_f}\right)\right)&\end{aligned} \tag{4}$$

The slip velocity $\vec{v}_{f,p}$ represents the velocity of the particles relative to base fluid and determined by Manninen *et al.* through Schiller and Naumann drag formulation as below;

$$\vec{v}_{f,p}=\vec{v}_p-\vec{v}_f=\frac{d_p^2\left(\rho_p-\phi_p\rho_p+\phi_f\rho_f\right)}{18\mu_f f_d\rho_p}\vec{a} \tag{5}$$

where $\vec{a}$ (particle's acceleration) and f_d are given as;

$$\vec{a}=\left(\frac{\phi_p\rho_p\vec{v}_p+\phi_f\rho_f\vec{v}_f}{\phi_p\rho_p+\phi_f\rho_f}\cdot\nabla\right)\frac{\phi_p\rho_p\vec{v}_p+\phi_f\rho_f\vec{v}_f}{\phi_p\rho_p+\phi_f\rho_f} \tag{6}$$

$$f_d=0.0183Re_p \qquad Re_p\geq 1000 \tag{7}$$

The particle Reynolds number is defined as;

$$Re_p=\frac{U_m d_p}{\mu_f}\left(\phi_p\rho_p+\phi_f\rho_f\right) \tag{8}$$

This study was performed using the realizable k- ε turbulence model with enhanced wall treatment. Relation $\mu_t=\rho C_\mu k^2/\varepsilon$ is used to combine the turbulent kinetic energy and turbulent dissipation rate. The turbulent kinetic energy and the turbulent dissipation rate at the tube inlet were obtained from Eqs. (9)-(10) and the initial assumption were computed using Eq. (11).

$$k=\frac{3}{2}(u\cdot I)^2 \tag{9}$$

$$\varepsilon=C_\mu^{3/4}\frac{k^{3/2}}{L} \tag{10}$$

$$I=\frac{0.16}{Re^{1/8}} \tag{11}$$

In this study TiO_2/water nanofluid is used and thermal properties relation are shown in Table 1.

Table 1. Thermo-physical properties of TiO_2 /water nanofluid

Thermo-physical property	Relation
Density (kg/m^3)	Mixture rule [1] $\rho_{eff}=\left(1-\emptyset_p\right)\rho_f+\emptyset_p\rho_p$

Specific heat (J/kg·K)	Thermal equilibrium [1] $c_{p,eff} = \frac{(1-\emptyset_p)\rho_f c_{p,f} + \emptyset_p \rho_p c_{p,p}}{\rho_{eff}}$
Viscosity (m Pa·s)	Einstein`s model [26] $\mu_{eff} = \mu_f(1 + 2.5\emptyset_p)$
Thermal conductivity (W/m·K)	Maxwell Garnett model [27] $k_{eff} = \frac{k_p + 2k_f - 2\emptyset_p(k_f - k_p)}{k_p + 2k_f + \emptyset_p(k_f - k_p)}$

3. RESULTS AND DISCUSSION

A numerical scheme was validated with the published experimental data [28] as shown in Figures 3 and 4. Figures 3 and 4 shown the swirl velocity and the profile of dimensionless temperature for the counter rotating case at *Re*=10000 respectively. It is clearly seen that the current simulation setup are in close agreement with the published experimental work [28].

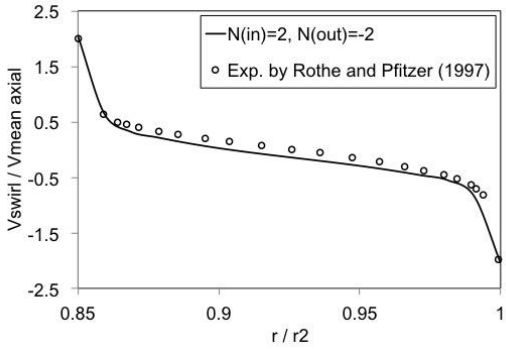

Figure 3. Profile velocity of swirl for counter-rotating case at *Re*=10000

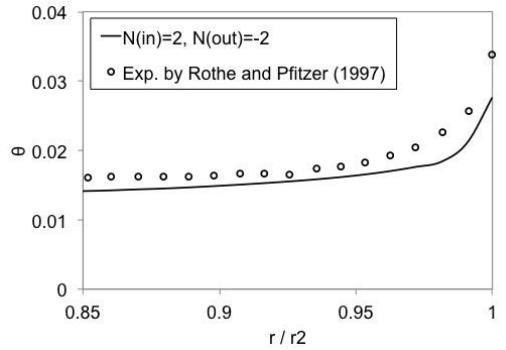

Figure 4. Profile of dimensionless temperature for counter-rotating case at *Re*=10000

Figures 5-7 shows the local Nusselt number distribution along the inner shaft for the counter rotating case. In Figure 5, the local Nusselt number for the 0.1 vol% TiO_2/water nanofluid at *Re* = 10000 is plotted.

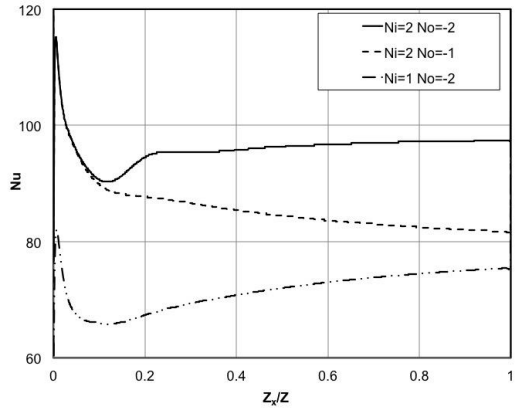

Figure 5. Local Nusselt number distribution along the inner shaft wall for the 0.1 vol% TiO_2/water nanofluid counter rotating case at *Re* = 10000

Figure 5 shows that the highest local Nusselt number is located at the tube inlet. The local Nusselt number gradually decrease towards the tube outlet. Later, at 10 percent of the total tube length from the inlet, behaviour of the local Nusselt number distribution is changed. Increase in the local Nusselt number is seen for the case of rotational speed of inner shaft is lower/equal than/to outer tube. While the local Nusselt number is decreased for the case of rotational speed of inner shaft is higher than outer tube.

At *Re*=5000 with the 0.1 vol% TiO_2/water nanofluid the local Nusselt number distribution for the varies rotational speed of the inner shaft and outer tube is shown in Figure 6.

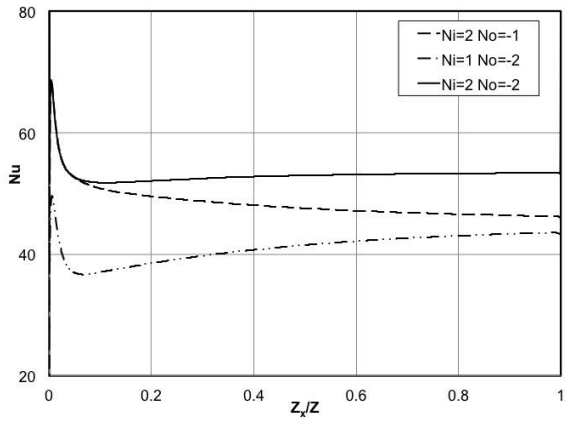

Figure 6. Local Nusselt number at the inner shaft wall for the 0.1 vol% TiO_2/water nanofluid counter rotating case at *Re* = 5000

Similar behaviour of the local Nusselt number distribution in Figure 5 is seen in Figure 6. The highest local Nusselt number for all cases is observed at the inlet. But, in overall the highest Nusselt number in Figure 6 is lower than Figure 5, this result is expected because of the Reynolds number in Figure 6 is less than the Reynolds number in Figure 5.

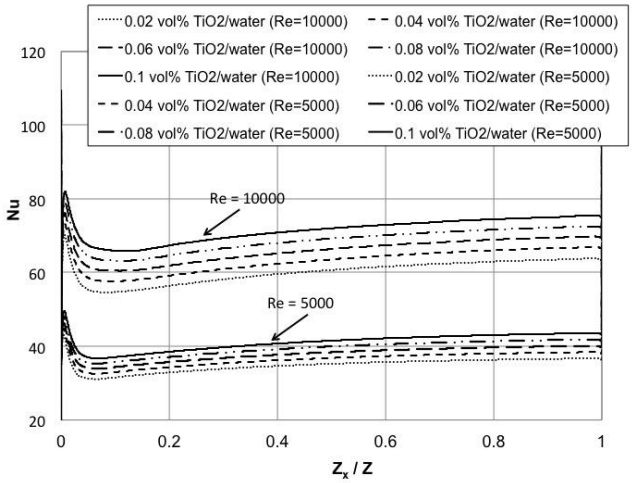

Figure 7. Local Nusselt number at the inner shaft wall for various volume percentages of TiO_2/water nanofluid at *Re*=10000 and *Re* =5000 (counter rotating case, Ni=1 No=-2)

Figure 7, show the local Nusselt number along the inner shaft for all cases at the Reynolds number of *Re*=5000 and *Re*=10000. The local Nusselt number profile along the tube is identical for both cases, where the highest local Nusselt number is observed at the inlet. Moreover, a significant effect of the nanoparticle concentration in the nanofluid is observed for *Re* =10000 case compared to *Re* =5000 case.

Figures 8-10 shows the local Nusselt number along the inner shaft wall for the co-rotating case.

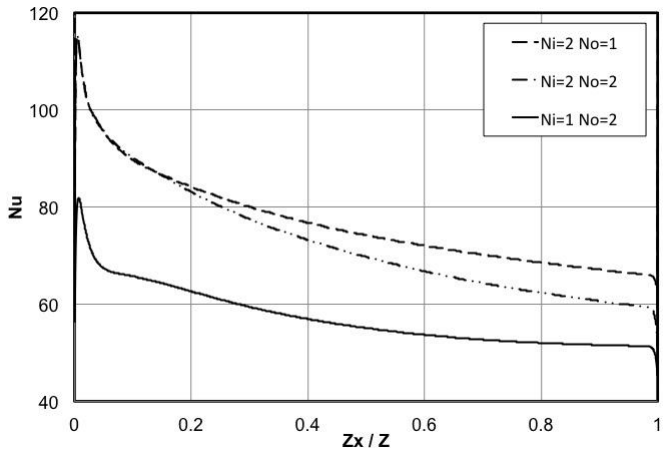

Figure 8. Local Nusselt number along the inner shaft wall for the 0.1 vol% TiO_2/water nanofluid co-rotating case at *Re* = 10000

It can be seen in Figure 8, that the maximum local Nusselt number is observed at the inlet and decreased gradually along the tube towards the outlet for all co-rotating cases. The lowest average Nusselt number is observed for the case of inner shaft rotate at the rotational speed lower than the outer tube. On the other hand, when the inner shaft rotated faster than outer tube the average Nusselt number is highest.

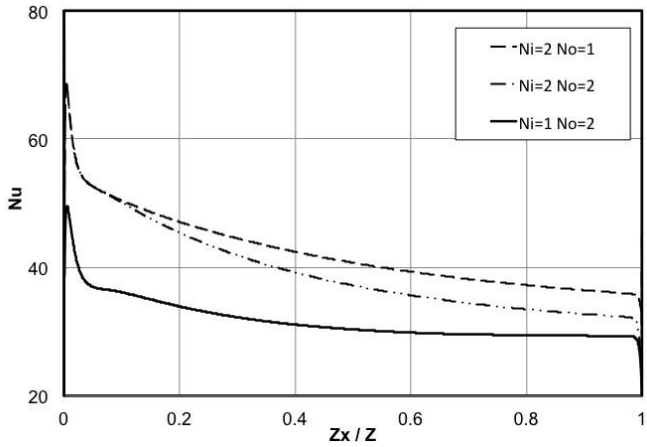

Figure 9. Local Nusselt number at the inner shaft wall for the 0.1 vol% TiO_2/water nanofluid co-rotating case at *Re* = 5000

In Figure 9, similar behaviour of the local Nusselt number along the inner shaft in Figure 8 is observed. Moreover, the average Nusselt number in Figure 9 is less than the average Nusselt number in Figure 8. These finding is similar to counter rotating cases in Figures 5 and 6 where the Reynolds number controlling the average Nusselt number.

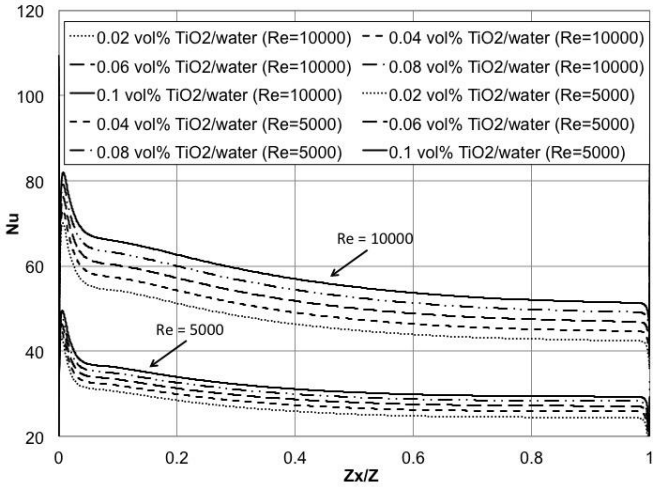

Figure 10. Local Nusselt number at the inner shaft wall for the various volume percentage of TiO_2/water nanofluid at *Re*=10000 and Re=5000 (co-rotating case, Ni=1 No=2)

An effect of the volume percentage of TiO_2/water nanofluid in co-rotating case at *Re*=10000 and Re=5000 is shown in Figure 10. At the Reynolds number of *Re*=10000, a significant effect of the particle concentration in the nanofluid is observed in comparison to *Re*=5000. Thus, in spite of the inner shaft and outer tube rotational speed, the effect of the volume percentage of nanofluid on the Nusselt number is significantly due to the Reynolds number.

Figure 11, shows a local Nusselt number along the inner shaft for the co-rotating and counter rotating cases with various inner shaft and outer tube rotation speed at *Re*=10000.

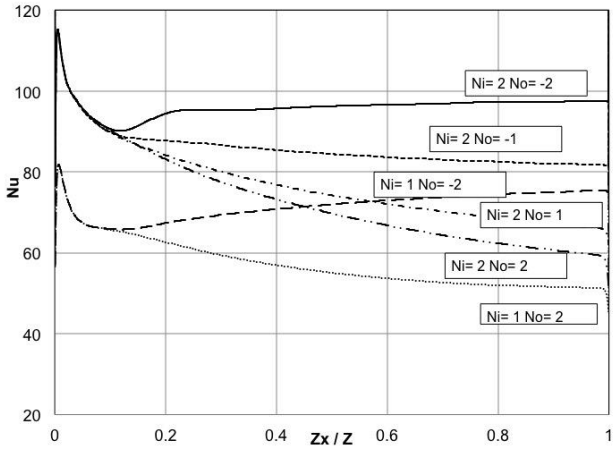

Figure 11. Local Nusselt number at the inner shaft wall for various inner shaft and outer tube rotation speed at *Re* = 10000

It is clearly seen that the highest average Nusselt number is produced by the counter rotating case with a same rotational speed of the inner and outer tubes. While the lowest average Nusselt number is observed for the co-rotating case with a rotational speed of inner shaft is lower than the outer tube. In overall, the counter rotating case produces higher average Nusselt number in comparison to co-rotating case. Moreover, effect of the inner shaft rotation speed is significant, increase in the rotational speeds of inner shaft increases the average Nusselt number. This observation is suppose due to the extra turbulences generated by competing rotational speeds between the inner shaft and outer tube. Furthermore, a sharp drop of the local Nusselt number at 10 percent entrance length for all cases was also observed. Beyond the 10 percent of the entrance length, a significant effect of the rotation direction between the inner shaft and outer tube and the rotational speed is seen. This is thought, to be caused by the boundary layers disturbances that source form the additional vortices produced by the inner shaft and outer tube rotation. The rotation of the inner shaft enhanced the turbulent kinetic energy and lead to a considerable increment of momentum and heat transfer.

7. CONCLUSIONS

The heat transfer behaviour of the TiO_2/water nanofluid flows inside annulus of finite rotating cylinders was successfully done. The distribution of local Nusselt number for *Re*=5000 and 10000 cases showed similarity at the tube entrance regions for both co-rotating and counter-rotating cases. It is also seen that an increase in vol% of the TiO_2 nanoparticle, increases the Nusselt number. The counter-rotating case with the rotational speed of outer tube is higher than the inner shaft was found to be more efficient in enhancing the heat transfer rate compared to the co-rotating case. While, the lowest average Nusselt number was observed for the co-rotating case with the rotational speed of outer tube is higher than the inner shaft. This observation is suggested due to the boundary layers disturbances and enhancement of the turbulent kinetic energy originated from the competing rotational speed between inner shaft and outer tube in the turbulent flow region.

ACKNOWLEDGMENT

The authors would like to be obliged to Universiti Pertahanan Nasional Malaysia for providing laboratory facilities.

REFERENCES

[1] Poncet S, Haddadi S, Viazzo S. (2011). Numerical modeling of fluid flow and heat transfer in a narrow Taylor-Couette-Poiseuille system, International Journal of Heat and Fluid Flow 32: 128-144. http://doi.org/10.1016/j.ijheatfluidflow.2010.08.003

[2] Viazzo S, Poncet S. (2014). Numerical simulation of the flow stability in a high aspect ratio Taylor-Couette flow submitted to a radial temperature gradient, Computer & Fluids 101: 15-26. https://doi.org/10.1016/j.compfluid.2014.05.025

[3] Stephen USC, Eastman JA. (1995). Enhancing thermal conductivity of fluids with nanoparticles, ASME International Mechanical Engineering Congress and Exposition, San Francis, pp. 1-8.

[4] Alawi OA, Sidik NAC, Mohammed HA, Syahrullail S. (2014). Fluid flow and heat transfer characteristics of nanofluids in heat pipes: A review, International Communications in Heat and Mass Transfer 56: 50-62. https://doi.org/10.1016/j.icheatmasstransfer.2014.04.014

[5] Leong KY, Nurfadhillah MH, Risby MS, Hafizah AN. (2016). The effect of surfactant on stability and thermal conductivity of carbon nanotube based nanofluids, Thermal Sciences 20: 429-436. https://doi.org/10.2298/TSCI130914078L

[6] Mousa MG. (2011). Effect of nanofluid concentration on the performance of circular heat pipe, Ain Shams Engineering Journal 2(1): 63-69. https://doi.org/10.1016/j.asej.2011.03.003

[7] Ting HH, Hou SS. (2015). Investigation of laminar convective heat transfer for Al_2O_3-water nanofluids flowing through a square cross section duct with a constant heat flux, Materials 8(8): 5321-5335. https://doi.org/10.3390/ma8085246

[8] Mahmoudi A, Mejri I, Omri A. (2016). Study of natural convection in a square cavity filled with nanofluid and subjected to a magnetic field, International Journal of Heat and Technology 34(1): 73-79. https://doi.org/10.18289/ijht.340111

[9] Motevasel M, Nazar ARS, Jamialahmadi M. (2017). Experimental investigation of turbulent flow convection heat transfer of MgO/water nanofluid at low concentrations – Prediction of aggregation effect of nanoparticles, International Journal of Heat and Technology 35(4): 755-764. https://doi.org/10.18280/ijht.350409

[10] Elahmer M, Abboudi S, Boukadida N. (2017). Nanofluid effect on forced convective heat transfer inside a heated horizontal tube, International Journal of Heat and Technology 35(4): 874-882. https://doi.org/10.18280/ijht.350424

[11] Roslan R, Saleh H, Hashim I. (2012). Effect of rotating cylinder on heat transfer in a square enclosure filled with nanofluids, International Journal of Heat Mass

Transfer 55(23–24): 7247-7256. https://doi.org/10.1016/j.ijheatmasstransfer.2012.07.051
[12] Khanafer K, Aithal SM. (2013). Laminar mixed convection flow and heat transfer characteristics in a lid driven cavity with a circular cylinder, International Journal of Heat Mass Transfer 66: 200-209. https://doi.org/10.1016/j.ijheatmasstransfer.2013.07.023
[13] Selimefendigil F, Öztop HF. (2014). Numerical study of MHD mixed convection in a nanofluid filled lid driven square enclosure with a rotating cylinder, International Journal of Heat Mass Transfer 78: 741-754. https://doi.org/10.1016/j.ijheatmasstransfer.2014.07.031
[14] Chatterjee D, Gupta SK, Mondal B. (2014). Mixed convective transport in a lid-driven cavity containing a nanofluid and a rotating circular cylinder at the center, International Communication in Heat and Mass Transfer 56: 71-78. https://doi.org/10.1016/j.icheatmasstransfer.2014.06.002
[15] Selimefendigil F, Öztop HF. (2015). Mixed convection in a two-sided elastic walled and SiO_2 nanofluid filled cavity with internal heat generation: Effects of inner rotating cylinder and nanoparticle's shape, Journal of Molecular Liquids 212: 509-516. https://doi.org/10.1016/j.molliq.2015.09.037
[16] Mustafa MF, Hayat T, Alsaedi A. (2016). Numerical study for rotating flow of nanofluids caused by an exponentially stretching sheet, Advanced Powder Technology 27(5): 2223-2231. https://doi.org/10.1016/j.apt.2016.08.007
[17] Sheikholeslami A, Ganji DD. (2014). Numerical investigation for two phase modeling of nanofluid in a rotating system with permeable sheet, Journal of Molecular Liquids 194: 13-19. https://doi.org/10.1016/j.molliq.2014.01.003
[18] Selimefendigil F, Öztop HF, Abu-Hamdeh N. (2016). Mixed convection due to rotating cylinder in an internally heated and flexible walled cavity filled with SiO_2–water nanofluids: effect of nanoparticle shape, International Communication in Heat and Mass Transfer 71: 9-19. https://doi.org/10.1016/j.icheatmasstransfer.2015.12.007
[19] Wang TS, Huang Z, Xi G. (2017). Entropy generation for mixed convection in a square cavity containing a rotating circular cylinder using a local radial basis function method, International Journal of Heat Mass Transfer 106: 1063-1073. https://doi.org/10.1016/j.ijheatmasstransfer.2016.10.082
[20] Das K. (2014). Flow and heat transfer characteristics of nanofluids in a rotating frame, Alexandria Engineering Journal 53(3): 757-766. https://doi.org/10.1016/j.aej.2014.04.003
[21] Turkyilmazoglu M. (2014). Nanofluid flow and heat transfer due to a rotating disk, Computer & Fluids 94: 139-146. https://doi.org/10.1016/j.compfluid.2014.02.009
[22] Hussain ST, Rizwan-ul- Haq, Khan ZH, Nadeem S. (2016). Water driven flow of carbon nanotubes in a rotating channel, Journal of Molecular Liquids 214: 136-144. https://doi.org/10.1016/j.molliq.2015.11.042
[23] Bowen RM. (1976). Theory of Mixtures, Part I. In: Eringen, A. C. (Ed.), Continuum Physics, vol. III. New York: Academic Press.
[24] Johnson G, Massoudi M, Rajagopal KR. (1991). Flow of a fluid-solid mixture between flat plate, Chemical Engineering Science 46(7): 1713–1723. https://doi.org/10.1016/0009-2509(91)87018-8
[25] Joseph DD, Lundgren TS, Jackson R, Saville DA. (1990). Ensemble averaged and mixture theory equations for incompressible fluid particle suspensions, International Journal of Multiphase Flow 16(1): 35–42. https://doi.org/10.1016/0301-9322(90)90035-H
[26] Einstein (1956). Investigation on the Theory of Brownian Motion, Dover, New York.
[27] J.C. Maxwell (1881). A Treatise on Electricity and Magnetism, second ed., Clarendon Press, Oxford UK.
[1] Rothe T, Pfitzer H. (1997). The influence of rotation on turbulent flow and heat transfer in an annulus between independently rotating tubes, Heat and Mass Transfer 32(5): 353-364. https://doi.org/10.1007/s002310050132

NOMENCLATURE

$\vec{a}$ particle's acceleration
c_p specific heat, J/kg K
d_H hydraulic diameter, m
h convective heat transfer, W/m2K
h_k sensible enthalphy, kJ/kg
k thermal conductivity, W/mK
L tube length, m
q heat flux
Re Reynolds number
p pressure, Pa
T temperature, K
v velocity, m/s
v_{dr} drift velocity, m/s

Greek symbols

ϕ volume fraction
μ dynamics viscosity, kg/ms
ρ density, kg/m3
η kinematic viscosity, m2/s

Subscripts

bf base fluid
eff effective
f base fluid
p particle
vol% volume percentage